U.S. Department of the Interior
Geological Survey

SELECTED DATA FOR SEDIMENT CORES COLLECTED IN CHESAPEAKE BAY IN 1996 AND 1998

Pattie C. Baucom, John F. Bratton, Steven M. Colman[1], and Jennifer M. Moore
U.S. Geological Survey
384 Woods Hole Rd.
Woods Hole, MA 02543

John King and Chip Heil
Graduate School of Oceanography
University of Rhode Island
Narragansett, RI 02882

Robert R. Seal II
U.S. Geological Survey
National Center MS 954
Reston, VA 20192

U.S. Geological Survey Open-File Report 01-194

[1] Corresponding author: scolman@usgs.gov

ABSTRACT

As part of a study of the recent history of the Chesapeake Bay ecosystem, one- to eight-meter long sediment cores were obtained from the mesohaline section of the Chesapeake Bay between the mouths of the Potomac and Rhode Rivers. The sediments consist of three lithofacies: coarse-grained channel deposits, restricted-estuary sands and muds, and open-estuary muds. Water content, biogenic silica, magnetic susceptibility, trace metals, and nutrients (carbon, nitrogen, and their isotopes) were measured in the cores. Biogenic silica, trace-metal, and nutrient data provide a strong basis for discussing past primary productivity and water-column anoxia in the bay.

INTRODUCTION

This report is part of an interdisciplinary research project designed to document paleoenvironmental changes in the Chesapeake Bay, as recorded in the sedimentary record (Cronin *et al.*, 1999). Because of its location near several metropolitan areas and its function as a natural resource, commercial shipping thoroughfare, and recreational area, maintaining and improving the water quality of Chesapeake Bay has become an increasingly important challenge. Understanding the history of Chesapeake Bay is important when differentiating between the long-term, natural variability of the bay and the impact of humans during the last several hundred years.

Chesapeake Bay is the largest and most productive estuary in the United States. Its watershed covers approximately 166,000 km^2 in Maryland, Virginia, Pennsylvania, Delaware, and New York. It is 322 km long and 20-40 km wide, with and average depth of less than 8 meters (maximum depth is 53 m). The bay is a dynamic and complex system that serves as a two-way filter for sediment, water, nutrients, and biological production. It is a depositional area for both river sediment and for sediment entering the bay from the ocean. Sediments that have accumulated in Chesapeake Bay contain physical, geochemical and fossil indicators that can be used to reconstruct past environmental conditions. The bay is a former river valley, drowned by the post-glacial rise in sea level. The average historical rate of submergence of the bay is 3.3 mm/yr (Hicks and Hickman, 1988), more than three times the global average rate of relative sea-level rise, contributing to the dynamic nature of the system.

This report presents sediment core descriptions, X-radiographs, and quantitative analytical data including water content, biogenic silica (BSi) content, magnetic susceptibility, trace-metal concentrations, stable isotope ratios, and total organic carbon and nitrogen contents for cores collected during the summer field seasons of 1996 and 1998 from five locations in Chesapeake Bay (Fig. 1, Table 1). Core descriptions, X-radiographs, and similar data for the 1996 cores are presented in Kerhin *et al.* (1998). Results based on biological proxies from the 1996 cores are also discussed in Cronin *et al.* (1999, 2000) and Karlsen *et al.* (2001).

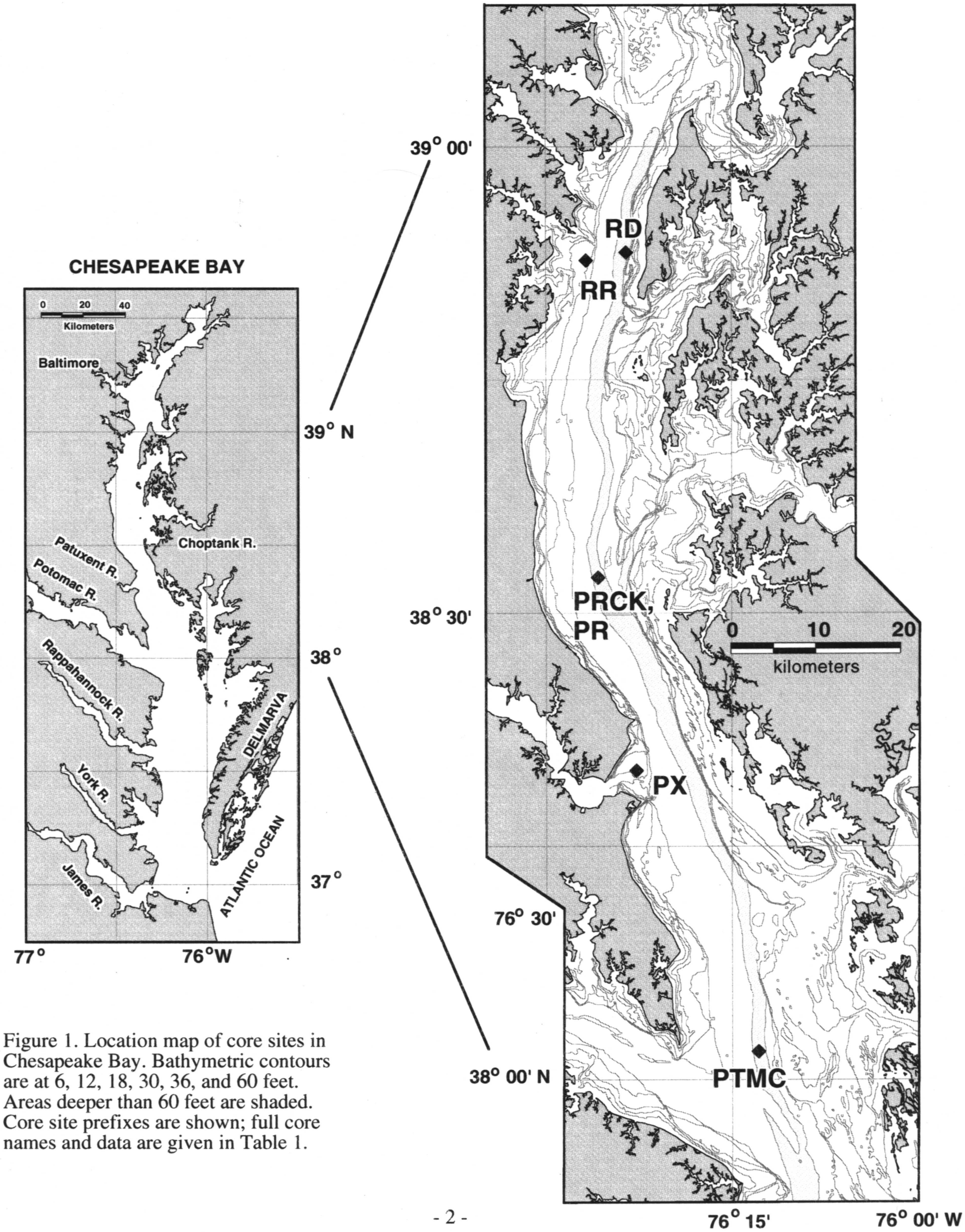

Figure 1. Location map of core sites in Chesapeake Bay. Bathymetric contours are at 6, 12, 18, 30, 36, and 60 feet. Areas deeper than 60 feet are shaded. Core site prefixes are shown; full core names and data are given in Table 1.

Table 1.-- 1996 and 1998 Chesapeake Bay Core Summary

Date	Location	Core	Water Depth (m)	Type	Latitude (°N)	Longitude (°W)	Length (cm)
1996	Potomac River	PTMC-3	23.1	Long Piston	38.6118	76.1938	450
1996	Deep Channel off Parker Cr.	PRCK-3	24.3	Long Piston	38.6349	76.6890	452
6/14/98	Deep Channel off Parker Cr.	PR98-1	21.8	Gravity	38.5382	76.4342	86
6/16/98	Deep Channel off Parker Cr.	PR98-2	21.9	Slow Piston	38.5378	76.4296	~457
6/16/98	Deep Channel off Parker Cr.	PR98-3	21.9	Slow Piston	38.5378	76.4296	97
6/16/98	Deep Channel off Parker Cr.	PR98-4	21.9	Long Piston	38.5377	76.4299	~427
6/17/98	Deep Channel off Parker Cr.	PR98-5	21.9	Mackereth	38.5378	76.4295	~150
6/17/98	Deep Channel off Parker Cr.	PR98-6	21.9	Mackereth	38.5378	76.4295	~150
6/11/98	Patuxent River Mouth	PX98-1	12.5	Gravity	38.3242	76.3897	105
6/16/98	Patuxent River Mouth	PX98-2	8.7	Long Piston	38.3311	76.3781	457
6/16/98	Patuxent River Mouth	PX98-3	8.7	Slow Piston	38.3311	76.3781	97
6/16/98	Patuxent River Mouth	PX98-4	8.7	Slow Piston	38.3311	76.3781	108
6/13/98	Rhode River Mouth	RR98-1	8.2	Gravity	38.8783	76.4406	105
6/15/98	Rhode River Mouth	RR98-2	8.9	Slow Piston	38.8790	76.4404	<100
6/15/98	Rhode River Mouth	RR98-3	7.9	Slow Piston	38.8776	76.4456	108
6/15/98	Rhode River Mouth	RR98-4	7.9	Slow Piston	38.8776	76.4456	109
6/15/98	Rhode River Mouth	RR98-5	7.9	Kasten	38.8776	76.4456	286
6/15/98	Rhode River Mouth	RR98-6	7.9	Long Piston	38.8776	76.4456	>400
6/15/98	Rhode River Mouth	RR98-7	7.9	Long Piston	38.8776	76.4456	446
6/15/98	Rhode River Mouth	RR98-8	7.9	Mackereth	38.8783	76.4406	500
6/16/98	Rhode River Mouth	RR98-9	7.9	Mackereth	38.8789	76.4399	780
11/1/98	Deep Channel off Rhode R.	RD98-1	26.0	Long Piston	38.8863	76.3947	459
11/1/98	Deep Channel off Rhode R.	RD98-2	26.0	Long Piston	38.8863	76.3947	~450
11/1/98	Deep Channel off Rhode R.	RD98-K1	26.0	Kasten	38.8863	76.3947	~300
11/1/98	Deep Channel off Rhode R.	RD98-K2	26.0	Kasten	38.8863	76.3947	~300

GEOLOGIC SETTING

The coastline and bathymetry of Chesapeake Bay reflect its origin as the drowned valley of the ancient Susquehanna River and its tributaries. As drowned river valleys, estuaries form when coastal plain river systems are inundated by rapid sea-level rise. The Chesapeake Bay is a classic example of an estuarine system shaped by a complex history of Quaternary sea-level fluctuations. Previous workers (Colman and Mixon, 1988; Colman *et al.*, 1990) used seismic-reflection surveys and boreholes to identify three generations of the Susquehanna River and three generations of Chesapeake Bay preserved as distinct paleochannel systems and their fills. Each of the paleochannel-fill sequences consists of two seismically distinguishable units. The lower sandy and gravelly fluvial unit is characterized by strong, irregular, discontinuous reflections, whereas the overlying fine-grained estuarine unit is characterized by weak, long, smooth reflections. The channel systems were formed during periods of low relative sea level and were backfilled with fine-grained estuarine sediment during subsequent sea-level highstands. The youngest paleochannel of the Susquehanna River preserved beneath Chesapeake Bay, called the Cape Charles system, was carved approximately 20,000 years ago and extended to the edge of the continental shelf (Colman *et al.*, 1990). Holocene sedimentary sequences partially or completely fill both the main axial channel of the Cape Charles paleochannel as well as the smaller tributary paleochannels, recording the post-glacial rise in sea level.

METHODS

Coring and Core Handling

At each of the 1996 coring sites, standard Kullenburg-type piston cores were obtained from the R/V Discovery (renamed the R/V Kerhin in 1999) using a 5-m-long core barrel containing a plastic liner with an inner diameter of 7 cm. Locations of the core sites were determined from standard Global Positioning System (GPS) signals in 1996 and from military-grade GPS in 1998 (Table 1).

In 1998, several additional Kullenburg-type piston cores were obtained, along with short, hydraulically damped piston cores and Kasten cores, from the R/V Discovery. In addition, long cores were obtained using a Mackereth-type piston coring device operated from a barge equipped with a crane (Fig. 2A). The crane raised the outer core barrel with the enclosed fiberglass inner core barrel to a vertical orientation and slowly lowered it to the sediment-water interface (Fig. 2B). Seawater was then pumped into the chamber above the inner core barrel to pressurize it and to drive the core barrel into the sediment. Once a core was successfully recovered, it was lifted back onto the barge, removed from the outer core barrel, labeled, capped and cut into 150-cm sections from bottom to top (Fig. 2C). Core recovery using this technique ranged from 102-776 cm.

After collection, cores were shipped to Woods Hole or to the University of Rhode Island and kept refrigerated until sediment physical properties could be measured and X-raying and sampling could be performed. Following measurements on a GEOTEK® multi-sensor track, cores

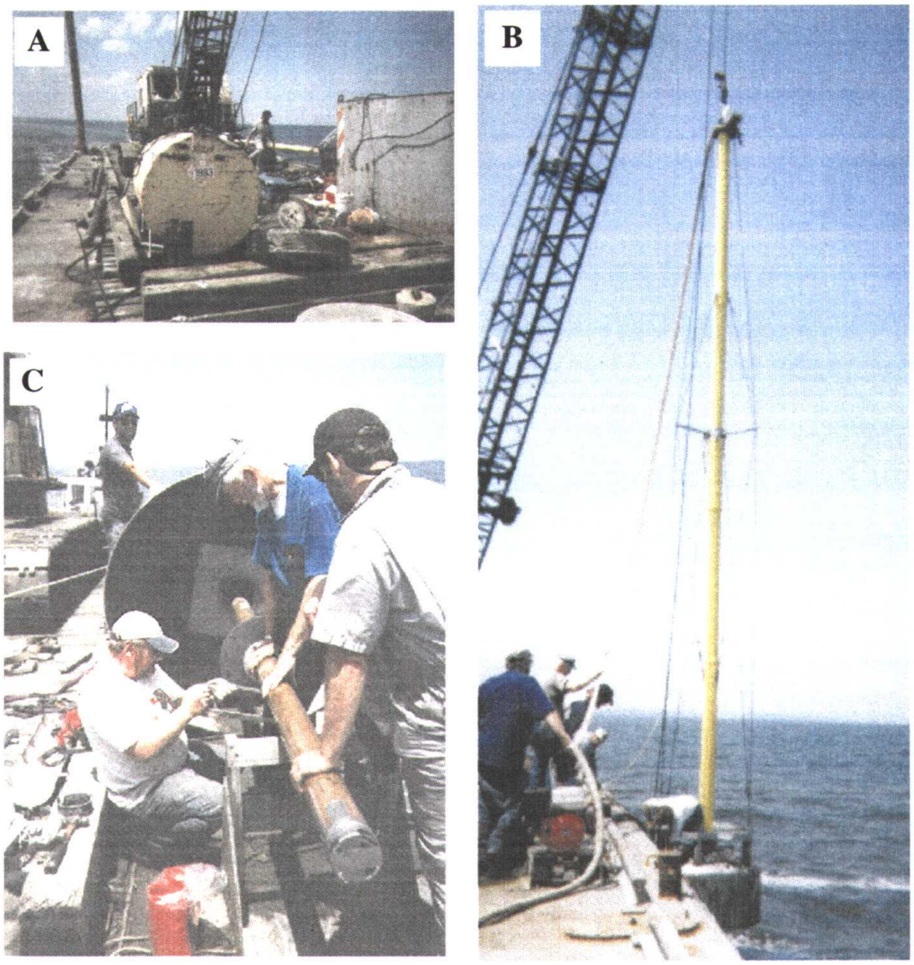

Figure 2. Photographs of the Mackereth coring operations.

were split longitudinally with a mechanical core-splitting device. Working and archive core halves were indicated with labels. The archive halves were used for sedimentological description, photography, and paleomagnetic analysis. The working halves were sub-sampled for water, biogenic silica, trace-metal, and isotope contents. Remaining sediment was bulk sampled for detailed paleontological analyses (foraminifera, ostracodes, diatoms, pollen and dinoflagellates). Typically, the entire working half was sampled in vials and plastic Whirl-pak bags, and the archive half was covered with plastic wrap, placed in a D-tube, sealed, and refrigerated for future reference or for additional scientific analyses.

Magnetic Susceptibility

Magnetic susceptibility (along with P-wave velocity and natural gamma-radiation attenuation, not discussed here) was measured on GEOTEK® multi-sensor track. Before the measurements were made, cores were allowed to equilibrate to room temperature. Plots of magnetic susceptibility against depth are shown in Figure 3. Where multiple cores were taken at the same site, the magnetic susceptibility data were used to correlate among the cores (Fig. 3) and develop a composite depth scale (Table 2). The original magnetic susceptibility data are included in Appendix A.

Core Description and X-radiographs

Sediment cores were described using standard sedimentological techniques, with emphasis on qualitative grain size, sedimentary structures, sediment color (based on Munsell® soil color charts), and biological components. Sediment grain size was described in detail using a 10X hands lens and a petrographic microscope. Smear slides were made at 50 to 100 cm intervals in order to investigate general changes in diatom abundance and to observe the preservation of diatom frustules. Mollusk shells and organic material were sampled for radiocarbon analysis. Detailed core descriptions are presented in Appendix B. X-radiographs were made for several of the cores described in this report. X-radiographs were helpful for detecting fossil burrows, shell material and laminations and banding that are not otherwise visible. Sedimentary structures (e.g. laminations) and biological components (e.g. shells) are labeled on X-radiographs of cores at the Rhode River sites in Figures 4 and 5, respectively. Lithologic descriptions and additional X-radiographs are in Appendix B.

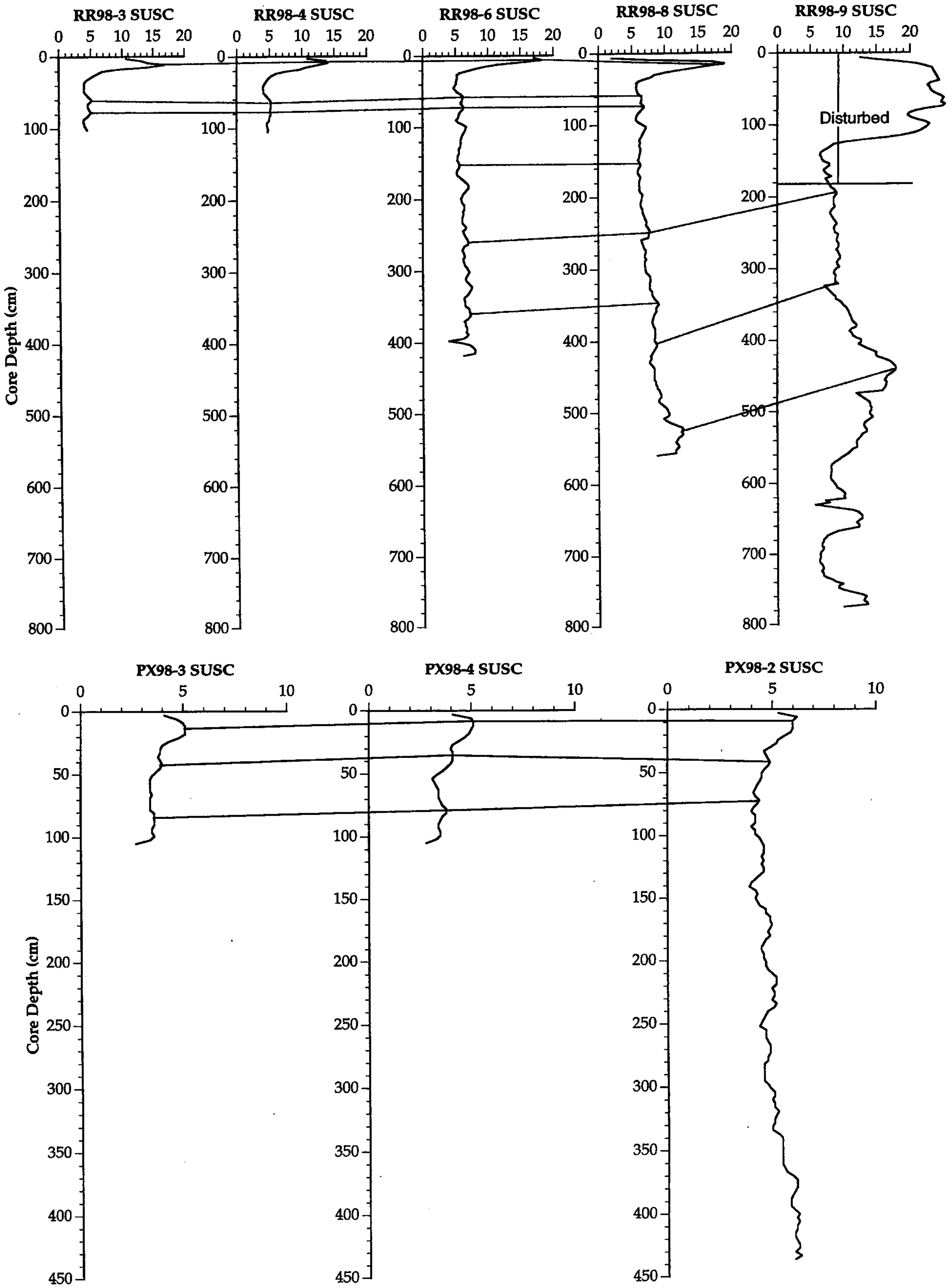

Figure 3. Plots of magnetic suseptibility (SI units) against depth for cores at the Patuxent River and Rhode River sites. Correlative horizons are shown by lines between cores.

Table 2. Correlation depths among cores at the Patuxent River and Rhode River sites, based on correlation of magnetic susceptibility profiles (Fig. 3)

Rhode River (RR)		Patuxent River (PX)	
Core and depth (cm)	Equivalent depth (cm) in RR98-8	Core and depth (cm)	Equivalent depth (cm) in PX98-2
RR98-3		PX98-3	
0	0	0	0
12	15	15	12
60	60	42	42
78	75	84	72
102	95	PX98-4	
RR98-4		0	0
0	0	9	12
9	15	36	42
66	60	78	72
81	75		
120	104.25		
RR98-6			
3	12.2		
6	15		
57	63		
72	75		
259	247		
361	349		
412	406		
RR98-9			
174	220.5		
195	247		
321	406		
441	523		
775	848.7		

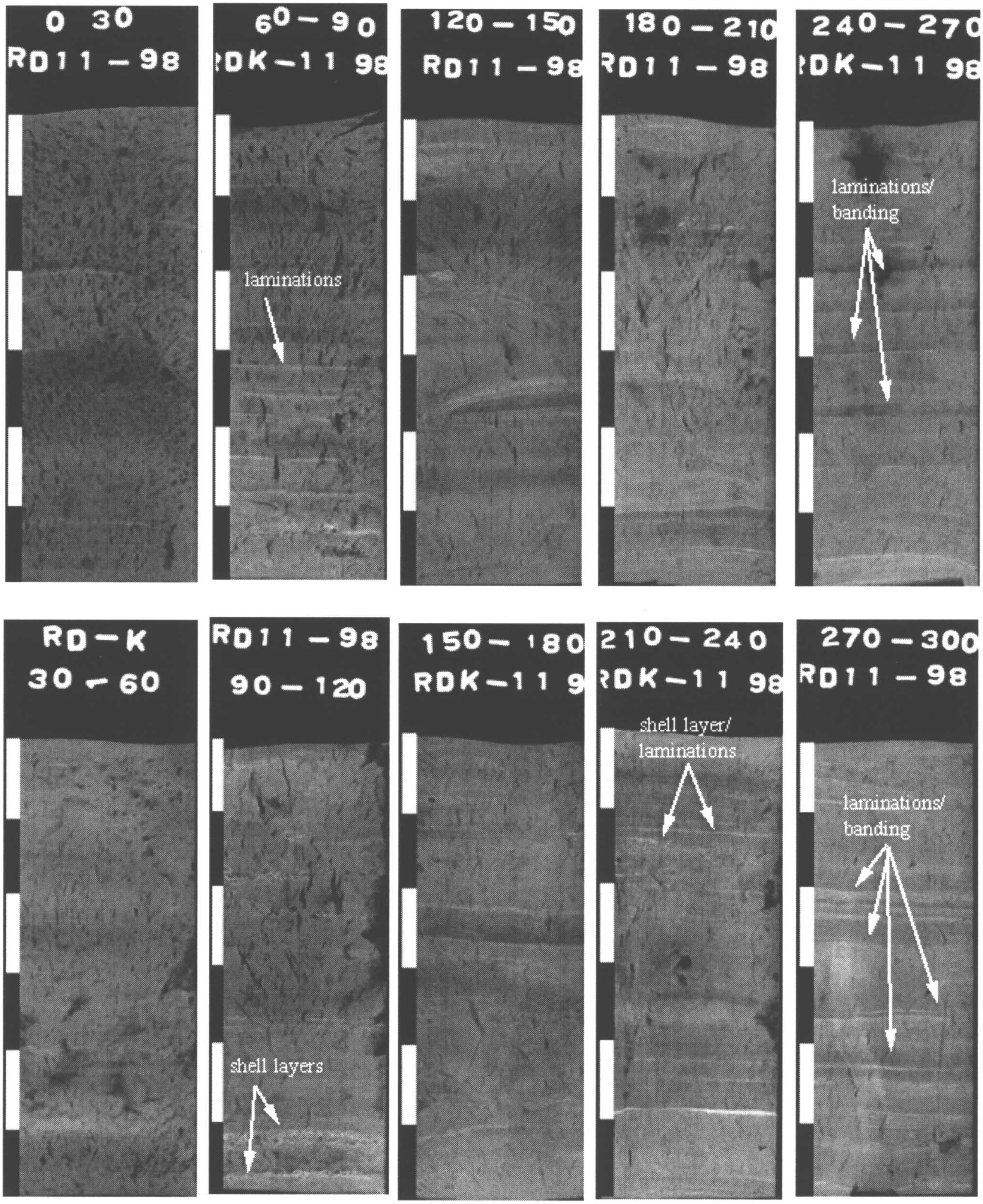

Figure 4. X-radiograph of sections of core RD98-K1 showing sedimentary structures. Core label and depth range are given at the top; scale divisions on left are 5 cm apart.

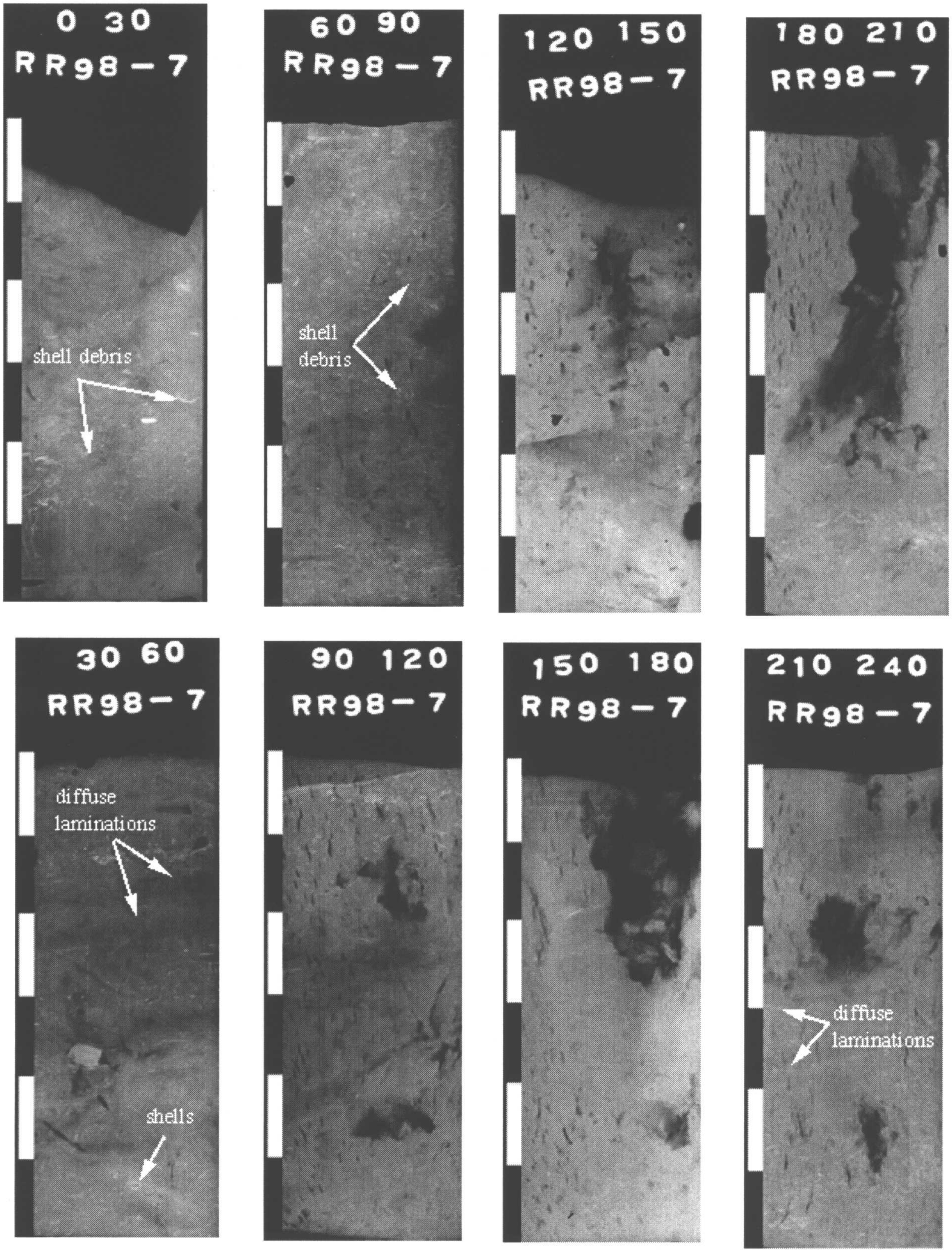

Figure 5. X-radiograph of sections of core RR98-K1 showing biological components of the sediments. Core label and depth range are given at the top; scale divisions on left are 5 cm apart.

Water Content Measurements

Water content measurements were taken at intervals of 10 and 3 cm in the 1996 and 1998 cores, respectively. After collection into sampling vials, each sediment sample was refrigerated until water content was measured. Samples were weighed while wet, dried at 60˚C for about three days, and re-weighed. Water content for each sample was calculated as follows:

$$(\text{wet sample mass} - \text{dry sample mass}) / (\text{wet sample mass}) * 100$$

Water-content data for 1996 and 1998 cores are included in Appendix C.

Biogenic Silica

Biogenic silica sample digestions were performed using methods modified slightly from those of Mortlock and Froelich (1989) as described by Carter and Colman (1994). Hydrogen peroxide (H_2O_2) and hydrochloric acid (HCl) solutions were added to samples to remove organic material and carbonate, respectively. Following these steps, 2N sodium carbonate solution (Na_2CO_3) was added to dissolve the biogenic silica within the sediment sample. Three milliliters of this solution were extracted from the sample, acidified, and analyzed by Inductively Coupled Plasma Atomic Emission Spectrometer (ICP-AES) for Si and Al. Raw ("uncorrected") biogenic silica measurements were corrected for clay-mineral dissolution using measured aluminum values and a Si:Al ratio of 1.76. This value was determined from the average of 8 analyses of the Si:Al ratio of fine-grained (<1 micron) clay from Chesapeake Bay sediments (Table 3). Biogenic silica content for 1996 and 1998 cores are included in Appendix D.

Table 3. Silica:Aluminum ratios in the fine clay fraction of Chesapeake sediments.

Sample	Size (m)	Al (ppm)	Si (ppm)	Si:Al
PTMC-3, 151a	0.5-1.0	1.59	2.95	1.85
PTMC-3, 151b	0.5-1.0	1.55	2.66	1.72
PTMC-3, 151c	0.5-1.0	1.85	3.51	1.90
Average of replicates above	0.5-1.0	1.66	3.04	1.82
PTMC-3, 151a	<0.5	1.27	2.06	1.62
PTMC-3, 311	0.5-1.0	1.43	2.38	1.67
PTMC-3, 311	<0.5	1.33	2.37	1.78
PRCK-3, 219	0.5-1.0	1.47	2.75	1.87
PRCK-3, 219	<0.5	0.93	1.70	1.82
Average		1.35	2.38	1.76

Trace Metals

Samples from the 1996 piston cores were analyzed for a suite of 23 metals including the redox-sensitive metals V, Zn, Cr, Ni and Cu as well as P, Fe, Mn Al, Ti, Ca, Mg, Na, K, Ba, Zr, Sr, Cd, Pb, Ag, Rb, Y and Se. Sediment samples were freeze-dried, ground to powder with mortar and pestle, and digested prior to analysis. Dried, ground samples were completely digested using a series of heated dissolutions and drydowns of approximately 50 mg of sediment in Teflon® vials containing mixtures of nitric acid, hydrofluoric acid, perchloric acid, and hydrogen peroxide to attack different solid phases (carbonate, metal oxides, silicates, organic matter) according to the protocol of Murray and Leinen (1996). Digested samples were diluted to appropriate concentrations (typically a 500-fold dilution) and analyzed by ICP-AES, and Graphite Furnace Atomic Absorption (GFAA) for some metals (Pb, Cd, Ag) at Boston University on instruments calibrated to standard solutions. Standard reference materials, replicates, method blanks, and reagents blanks were also prepared and analyzed with sample batches to monitor instrument and method accuracy and precision and to detect any significant sample contamination. Trace metal data for the 1996 cores are available in Appendix E. Analyses of other redox-sensitive metals (U, Mo) from the 1998 cores are in progress at Woods Hole Oceanographic Institution.

For rhenium analyses, dried and powdered sediment samples (~ 0.1 g) were mixed with 1.5 ml 4N Seastar HNO_3 and allowed to react for one hour at room temperature to leach authigenic rhenium from samples. Sample vials were centrifuged and the supernatant was filtered using dedicated syringes and 0.45- m cartridge filters. Leachate was combined with 0.1 g of 1.8-ppb ^{187}Re-enriched spike solution, diluted with Milli-Q   water 3-6 , and transferred to autosampler vials. Samples were analyzed by Inductively Coupled Plasma-Mass Spectroscopy (ICP-MS) using a Finnigan   Element 2 instrument equipped with an MCN6000 nebulizer and an autosampler maintained by Woods Hole Oceanographic Institution. Original sample concentrations were calculated from measured ratios of ^{187}Re:^{185}Re by the standard isotope dilution formula. Results are reported in Appendix F.

Isotopes, Total Organic Carbon, and Total Nitrogen

Carbon and nitrogen compositions, both bulk contents and isotopic values, were determined using a Carlo Erba   NC2500 Elemental Analyzer coupled to a Finnigan   Delta Plus isotope ratio mass spectrometer at the USGS facilities in Reston, Virginia. Total organic carbon (TOC) and total organic nitrogen (TN) determinations were calibrated using a marine sediment standard, the National Research Council of Canada Certified Reference Material PACS-2, with values of 3.32 mass percent C and 0.27 mass percent N. Carbon isotope compositions were measured on CO_2 and are reported in the   -notation, as permil (‰) relative to Vienna Pee Dee Belemnite (VPDB). The ^{13}C values are calibrated on a scale defined by USGS-24 (graphite) with ^{13}C = -15.9 ‰. Analytical precision is estimated to be ± 0.2 ‰ (1). Nitrogen isotope compositions were made on N_2 and are reported in the -notation, as permil (‰) relative to atmospheric N_2. The ^{15}N values are calibrated on a scale defined by an internal laboratory reference material G-3646 (acetanilide) with ^{15}N = -1.7 ± 0.1 ‰, which in turn, is referenced to a scale defined by IAEA-N1 (ammonium sulfate) with ^{15}N = 0.43 ‰ and USGS-32 (potassium nitrate) with ^{15}N = 180 ‰ (Böhlke and Coplen 1993). Analytical precision is estimated to be ± 0.2 ‰ (1).

Carbonate ^{13}C of foraminifera was determined by reacting 1-3 individual tests from each productive interval in a Kiel Device and measuring isotope ratios of evolved CO_2 with a Finnigan MAT 252 mass spectrometer operated by the Paleoceanography Research Group at the Woods Hole Oceanographic Institution. Results are reported relative to the Pee Dee Belemnite standard (PDB). Calibration and precision of this instrument are described in Ostermann and Curry (2000).

RESULTS

Magnetic Susceptibility

Magnetic susceptibility is generally interpreted as a proxy for the concentration of fine-grained magnetite in sediments, although post-depositional alteration and magnetic domain states also affect the measurement (Reynolds and King, 1995). Susceptibility is relatively high in the upper parts of most cores, but is relatively low and varies little in the underlying open-estuary muds (Fig. 3). This is consistent with more rapid deposition of sediment in post-settlement times, when soil erosion from agricultural fields would have contributed relatively fine-grained, pedogenic magnetite. In core RR98-9, the lower part of the section shows larger variations in magnetic susceptibility, associated with lithologic changes in the restricted-estuary and basal channel facies.

Magnetic susceptibility shows comparable fluctuations among cores taken at the same site (Fig. 3), and can be used to correlate among the cores. This is especially important for the RR site, where the upper part of core RR98-9 was disturbed during the coring operation.

Sedimentology

The sediments preserved beneath Chesapeake Bay record at least three lithofacies. These lithofacies include lithofacies OE (open-estuary) mud, lithofacies RE (restricted-estuary) sand and mud, and lithofacies C (channel deposits). Typically, only lithofacies OE was recovered using Kullenburg-type piston coring techniques. All lithofacies were recovered at the Rhode River site using the Mackereth corer (core RR 98-9, Fig. 6). Lithofacies OE is at least 410 cm thick at the Rhode River site and is composed of black to greenish gray, massive to diffusely laminated, slightly sandy (trace to ~10%), clayey mud. Filled burrows are common in the lower 100 cm of the lithofacies and broken and articulated bivalves are abundant throughout.

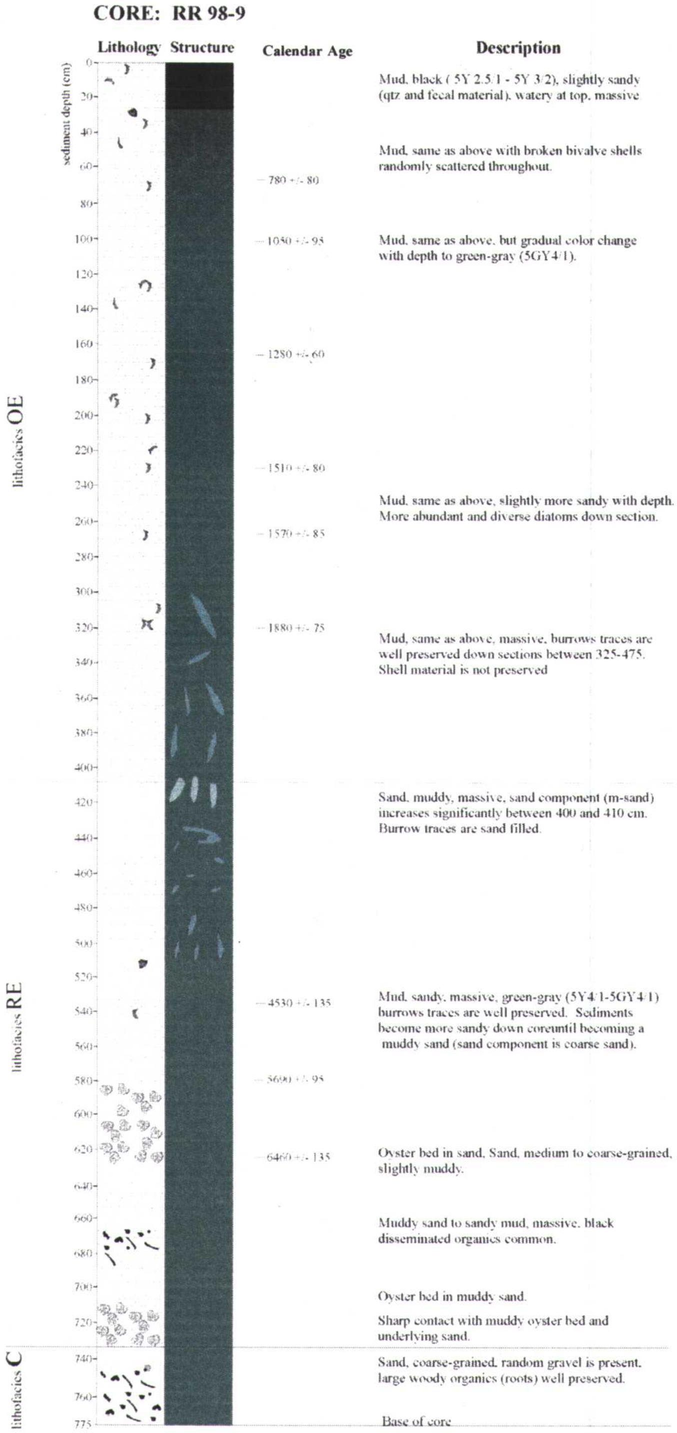

Mud, black (5Y 2.5/1 - 5Y 3/2), slightly sandy (qtz and fecal material), watery at top, massive

Mud, same as above with broken bivalve shells randomly scattered throughout.

Mud, same as above, but gradual color change with depth to green-gray (5GY4/1).

Mud, same as above, slightly more sandy with depth. More abundant and diverse diatoms down section.

Mud, same as above, massive, burrows traces are well preserved down sections between 325-475. Shell material is not preserved

Sand, muddy, massive, sand component (m-sand) increases significantly between 400 and 410 cm. Burrow traces are sand filled.

Mud, sandy, massive, green-gray (5Y4/1-5GY4/1) burrows traces are well preserved. Sediments become more sandy down coreuntil becoming a muddy sand (sand component is coarse sand).

Oyster bed in sand, Sand, medium to coarse-grained, slightly muddy.

Muddy sand to sandy mud, massive, black disseminated organics common.

Oyster bed in muddy sand.

Sharp contact with muddy oyster bed and underlying sand.

Sand, coarse-grained, random gravel is present, large woody organics (roots) well preserved.

Base of core

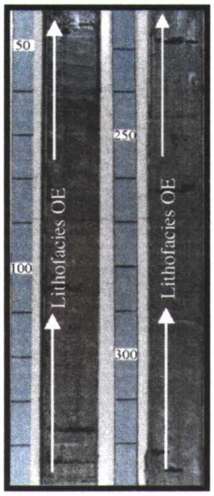

Photograph of lithofacies OE in core RR 98-9.

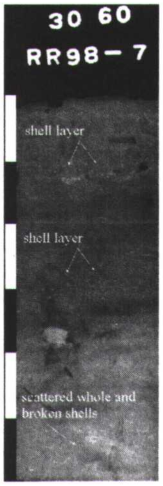

X-radiograph of the upper portion of lithofacies OE. Notice the scattered shells and shell layers.

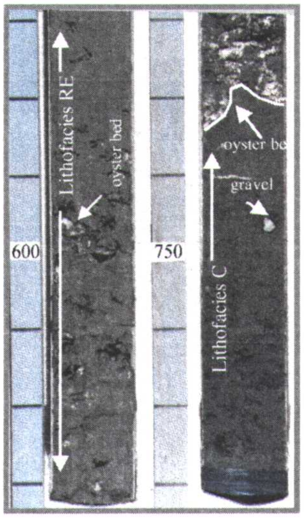

Photograph of lithofacies C overlain by lithofacies RE. Notice the oyster bed (from lithofacies RE) directly atop fluvial sand and gravel.

Lithofacies OE:

Lithofacies OE (open estuarine mud) is the youngest lithofacies preserved in Chesapekae Bay. It is approximately 410 cm thick and composed of black to greenish gray, massive to diffusely laminated, slightly sandy (trace to ~10%), clayey mud. Filled burrows are common in the lower 100 cm of this lithofacies and broken and articulated bivalves are abundant throughout this lithofacies.

Lithofacies RE:

Lithofacies RE (restricted estuarine mud and sand) is approximately 320 cm thick and is composed of greenish-gray, generally fining-upward, massive, poorly-sorted muddy sand to sandy mud with scattered oyster beds ranging from 15 to 40 cm thick. Woody organic layers are common. Filled burrows are well-preserved in the upper 100 cm of this lithofacies.

Lithofacies C:

Lithofacies C (channel sand) is approximately 50 cm thick and is composed of dark, greenish-black, massive, moderately sorted, quartzose medium- to coarse-grained pebbly sand. Gravel is present, but rare. Organic particles, mostly roots and leaves, are abundant and well preserved within lithofacies C.

Figure 6. Core log, descriptions, and X-radiographs of core RR98-9 showing the three lithologic facies observed in the sediments.

Lithofacies RE is at least 320 cm thick at this site and is composed of greenish-gray, generally fining-upward, massive, poorly-sorted muddy sand to sandy mud with scattered oyster beds ranging from 15 to 40 cm thick. Woody organic layers are common. Filled burrows are well-preserved in the upper 100 cm of this lithofacies. Lithofacies C was only recovered in core RR 98-9. It is approximately 50 cm thick and is composed of dark, greenish-black, massive, moderately sorted, quartzose medium- to coarse-grained sand. Gravel is present, but rare. Organic material, mostly roots and leaves, are abundant and well-preserved within lithofacies C.

Water Content

Sediment recovered in these cores contains between 40 and 70 percent water. The water-content data (Fig. 7) show two distinct relationships: (1) water content decreases with increasing sediment depth, and (2) water content decreases with increasing grain size. The first trend is due to sediment compaction (Fig. 7), and the only exceptions to the trend are the shallow-water sites (core PX98-2 and core RR98-9), where the upper 60 cm of the cores are sandy. Water content at these sites decreases upwards within sandier intervals (Fig. 7). The relationship between water content and grain size (qualitatively described from hand-lens observations) is strong enough that the water-content data is a useful guide to qualitative grain-size descriptions. Overall, grain-size variations in the OE and RE facies is quite small – most of the sediment is sandy to silty mud.

Biogenic Silica

Biogenic silica (BSi), a proxy for diatom productivity, was measured at all five sites within the middle part of Chesapeake Bay. The BSi data should record changes in total diatom productivity, either natural or in response to anthropogenic increases in nutrient discharge (fertilizers, municipal waste, nutrients in eroded soils). Diatoms were particularly useful for this type of study because their siliceous frustules are well-preserved in the sediments and they represent about 80-90% of the spring algal biomass (Cooper, 1995). However, several assumptions must be made when interpreting BSi data in terms of diatom productivity. The majority of the amorphous silica in the sediments is assumed to be in the form of diatom frustules rather than from other sources. Diatoms preserved in the sediments must also be considered representative of total diatom productivity. Little post-depositional dissolution of silica is assumed to have taken place, consistent with smear-slide observations that diatoms are well preserved in the sediments.

The overall bay-wide variation of BSi in the fine-grained estuarine sediments, is relatively low (4-12 percent), with short-term fluctuations of ±2 percent (Fig. 8). At shallow-water sites (PX98, RR98), biogenic silica has been rather low and fairly consistent with only minor changes in BSi concentration during the past few hundred years. However, at the deep-water sites (PTMC-3, RD98-1), where true open-estuarine muds are preserved and qualitative grain-size variations are smaller, BSi shows either no trend (PTMC-3) or a minor decrease in diatom productivity followed by a slight increase at the top of the core (RD98-1). Because there

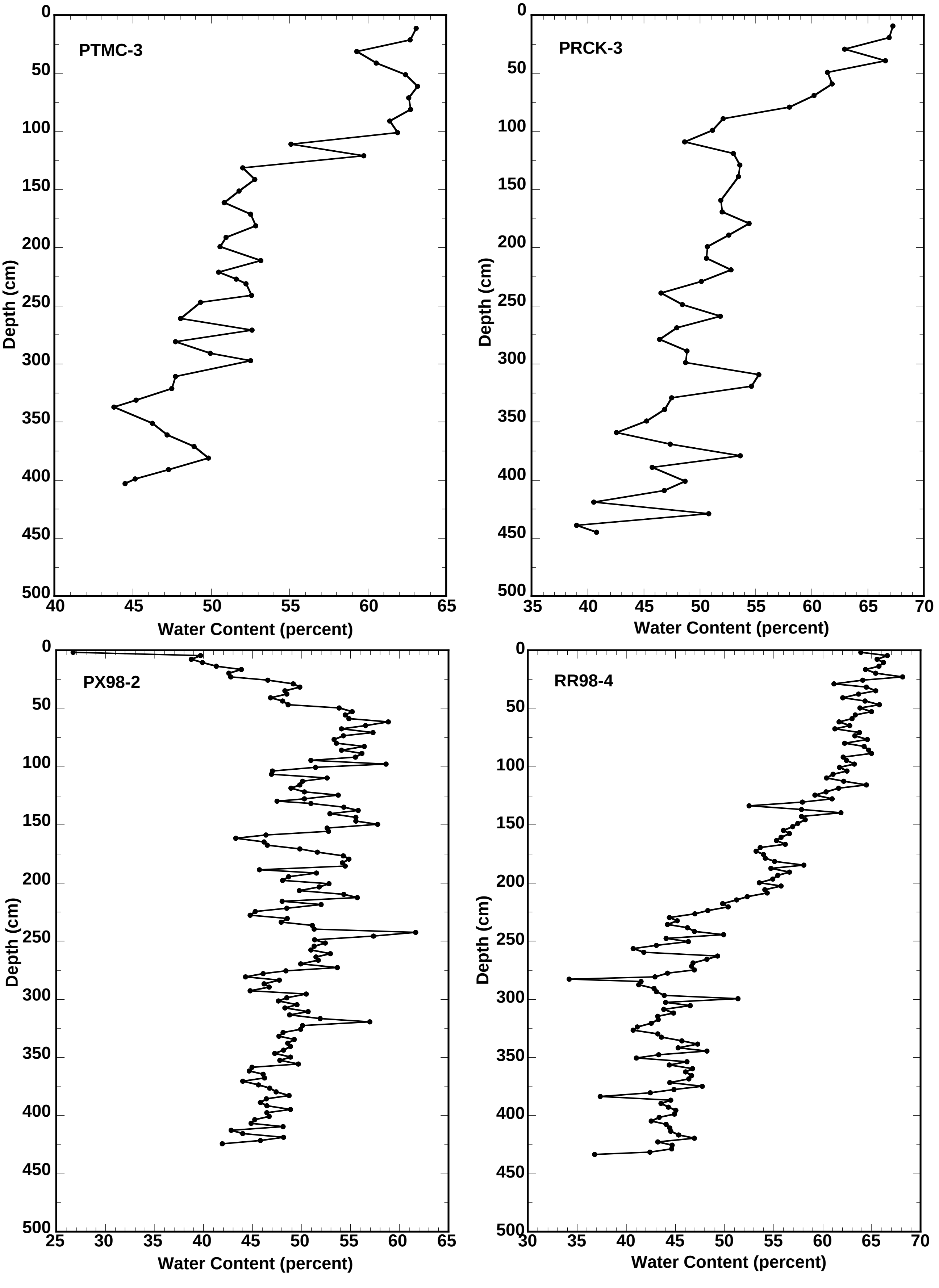

Figure 7. Plot of water content against depth for the cores in which water content was measured. For the RR site, the data are plotted on a common (corrected) depth scale derived from Figure 3 and given in Table 2.

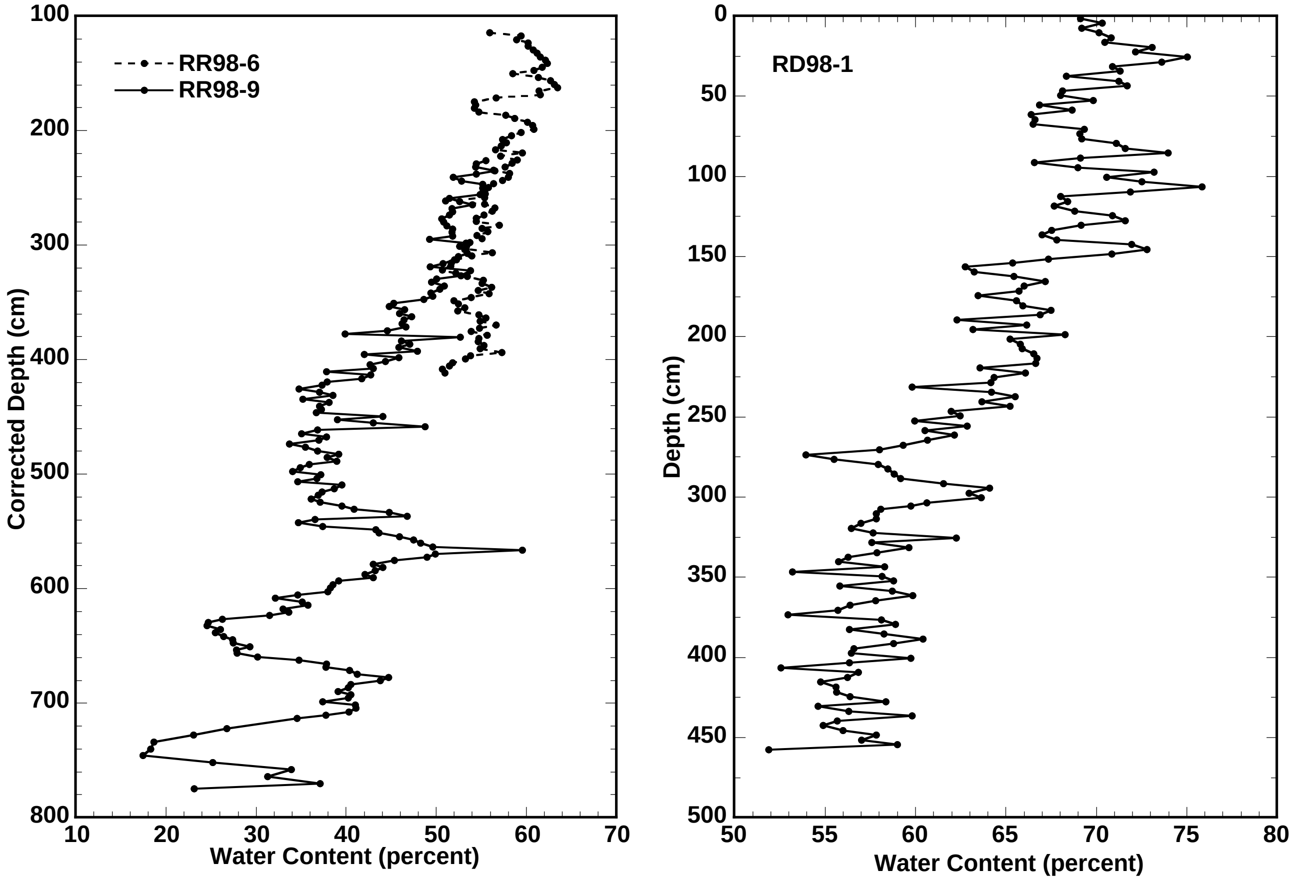

Figure 7. Continued.

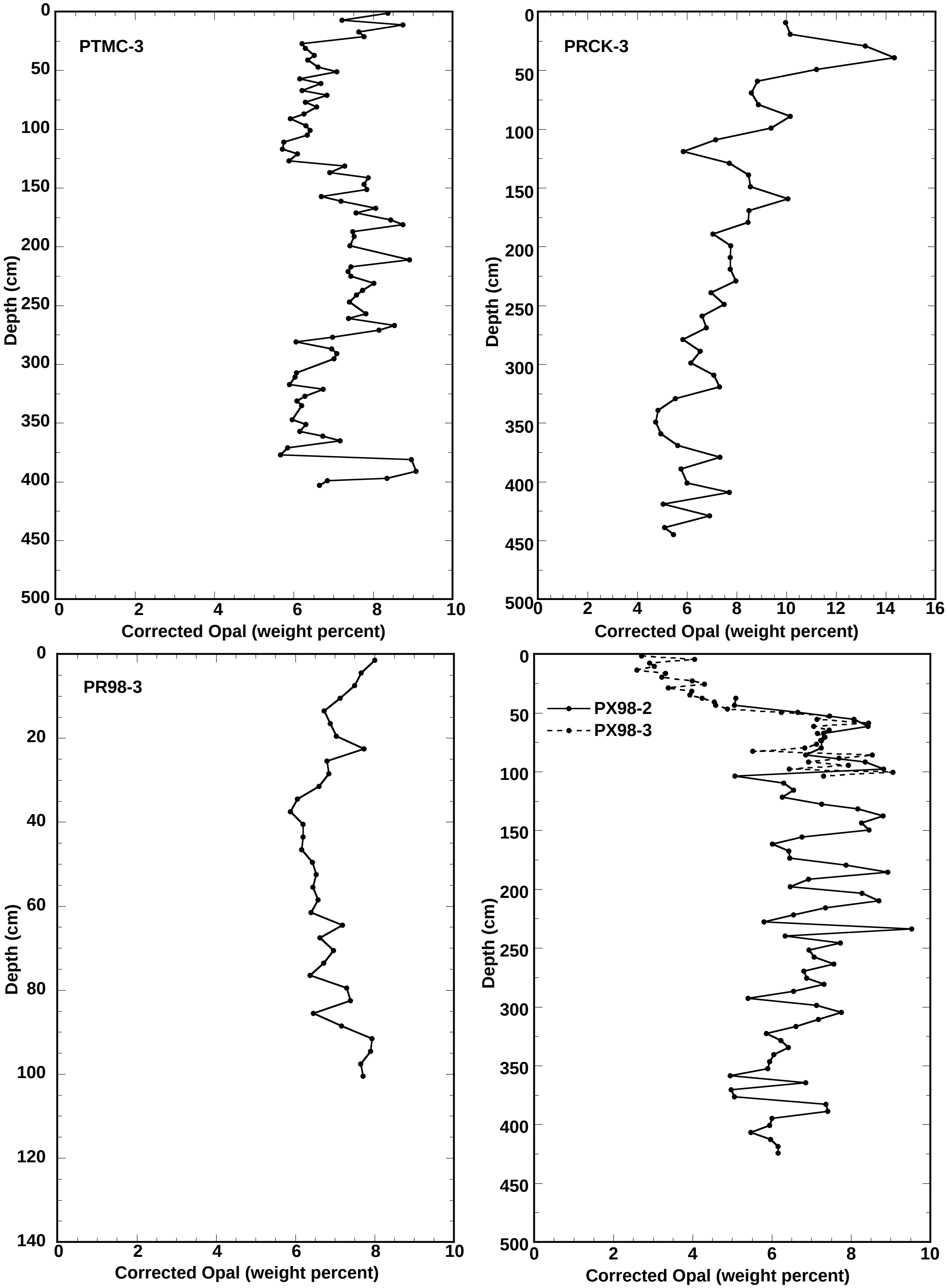

Figure 8. Plot of biogenic silica content against depth for the cores in which water content was measured. Biogenic silica values are corrected for clay-mineral dissolution (see text). For the RR site, the data are plotted on a common (corrected) depth scale derived from Figure 3 and given in Table 2.

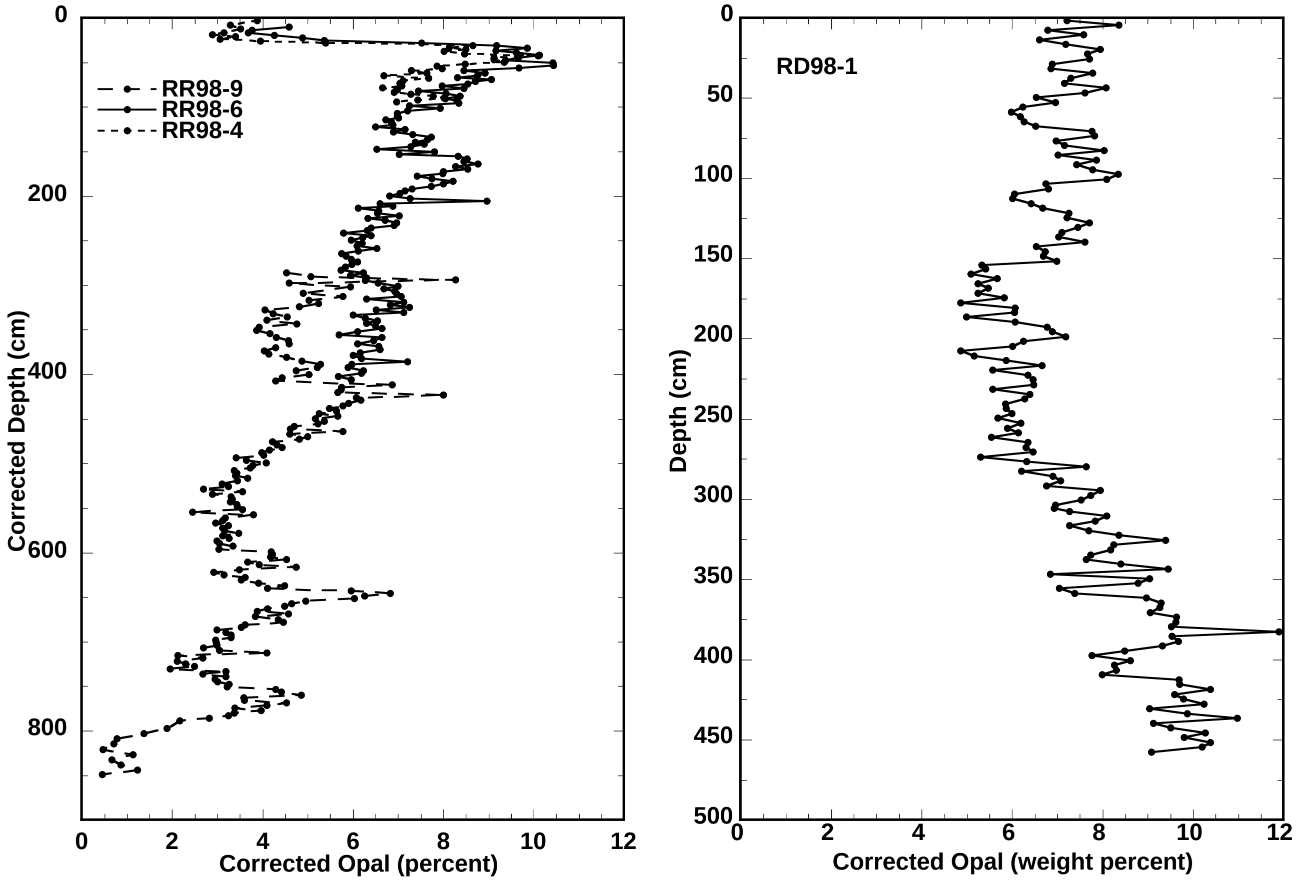

Figure 8. Continued.

was a large increase in sediment accumulation rates at these sites (Colman *et al.*, 2000; Willard and Korejwo, 2000) and other sites (Brush, 1986; Cooper and Brush, 1991, 1993) at about the time of initial land clearance (about 1800 AD), constant or increasing BSi concentrations imply equally large increases in the mass flux of biogenic silica.

Trace Metals

Samples from the 1996 cores (PRCK-3 and PTMC-3) were analyzed for a suite of 23 metals, as described above, including redox-sensitive metals (V, Zn, Cr, Ni, Cu). Trends of V, Zn, Cr, Ni, and Cu concentrations in the cores are consistent with those of other proxies, such as nitrogen isotopes (see below). Higher solid-phase concentrations of these metals indicate reducing conditions in the water column and shallow sediments that develop during longer and more intense summer anoxic periods. V, Zn, and Cr in particular are elevated in both cores above a depth of about 150 cm (Fig. 9). The signal is stronger at the northern (PRCK-3) site, possibly because of greater proximity to the Susquehanna River mouth and longer typical duration of summer anoxia at this site. The five metals shown co-vary in each core and correlate well between the two cores (Fig. 9). All are enriched above 150 cm in the cores (approximately 1750 A.D.), indicating increasing oxygen depletion in the bay after this time. Normalization of the data by plotting ratios of the metals to Al or Ti shows that the trends observed are not strongly influenced by the small grain-size variations in the upper parts of the cores. The Zn profile from PTMC-3 shows an anomalously large increase above 150 cm in the core.

Dissolved rhenium (Re) is unusually enriched in seawater relative to crustal abundances, but concentrations are still extremely low (<50 ppb). Dissolved Re becomes insoluble under reduced oxygen (but not necessarily anoxic) conditions and precipitates as a leachable authigenic sedimentary phase. If the sedimentation rate is known and the low Re concentration can be accurately measured, rhenium flux to sediment can be calculated as an indicator of relative duration and intensity of bottom water anoxia. By combining Re flux with other proxies such as ^{15}N and BSi flux, changes in the lower, middle, and upper layers of the Chesapeake water column can be determined. An example of this is shown in Figure 10, where data for core RD98-1 show that a gradual increase in diatom productivity began in about 1750 A.D. This increase resulted in oxygen depletion in the lower part of the stratified summer water column, producing ^{15}N enrichment and increased Fe flux to the sediment. These trends all increased sharply at about 1910 A.D., possibly related to construction of dams on the Susquehanna River.

Nitrogen Isotopes and Total Nitrogen

Total nitrogen (TN) and ^{15}N data for the five cores analyzed are reported in Appendix F. Values of TN for deep-water cores (RD98-2, PRCK-3, PTMC-3) decrease from a range of 0.23-0.33% near the core tops to a range of 0.10-0.12% at sediment depths greater than 4 m. This amounts to a downcore decrease of 50-70%. There is no obvious seaward trend in TN values among deep-water cores. Shallow-water values (cores RR98-6 and PX98-2) are lower (0.11 to

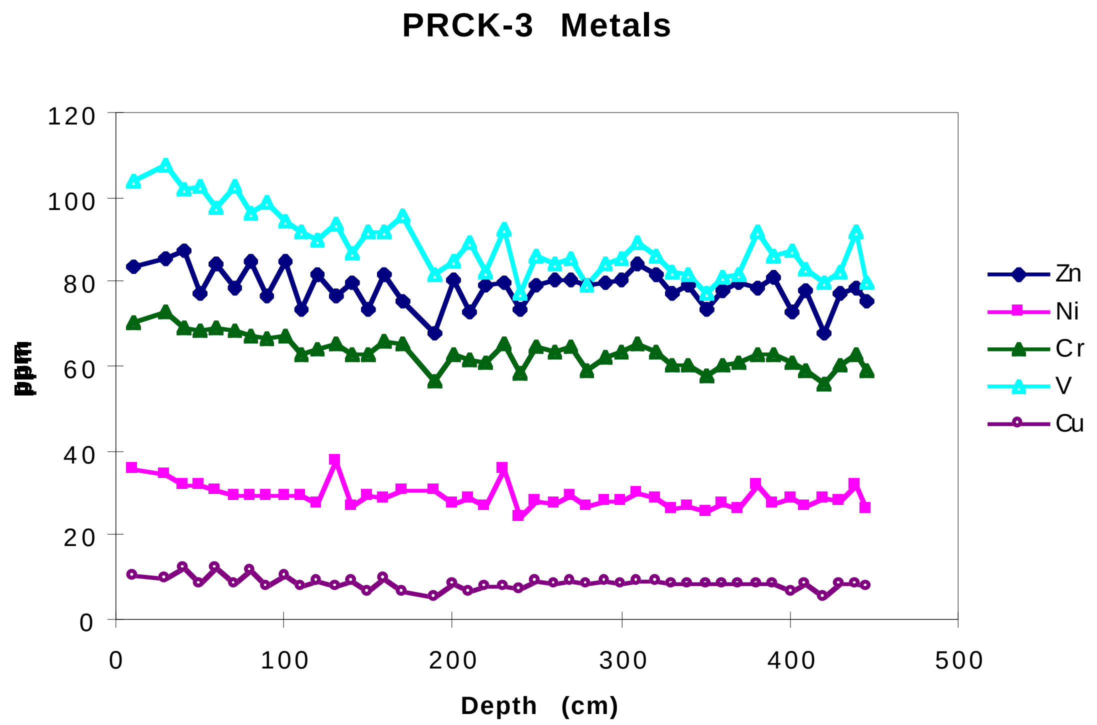

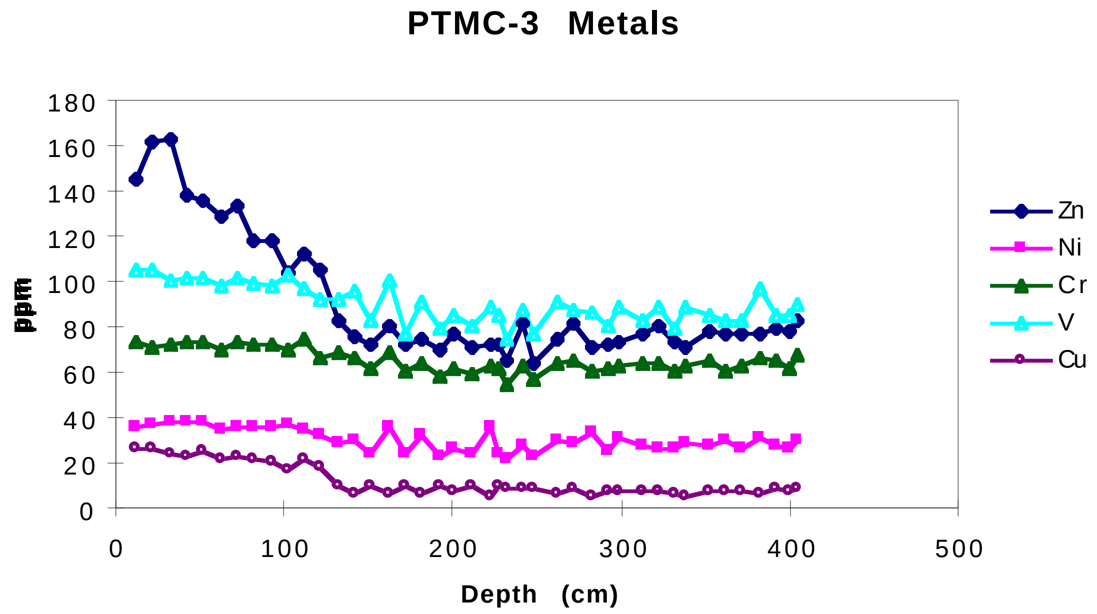

Figure 9. Selected trace metal contents plotted against depth for the 1996 cores, PRCK-3 (top) and PTMC-3 (bottom).

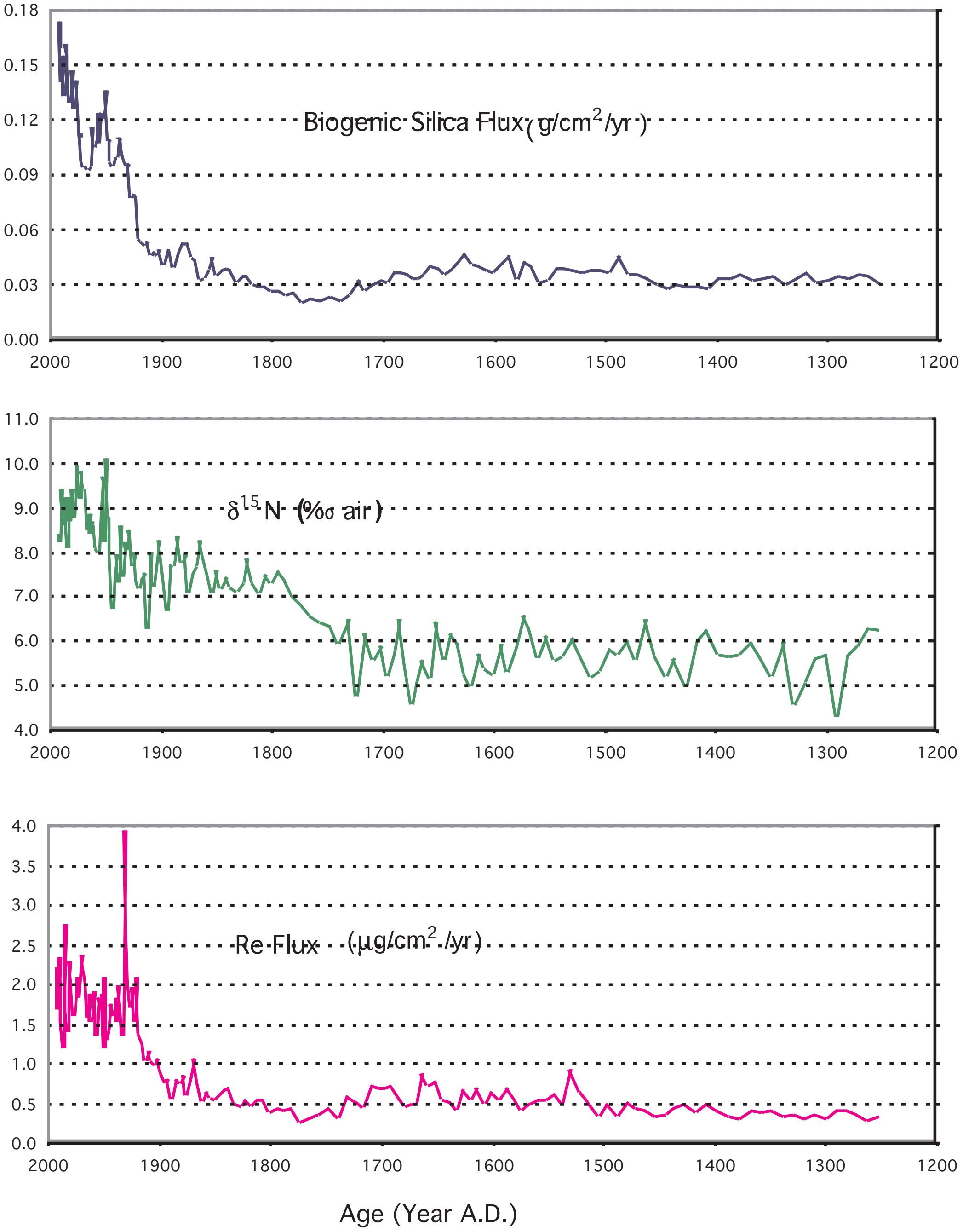

Figure 10. Plot of biogenic silica flux, nitrogen isotopes, and rhenium flux against age for core RD98-2. Age scale and flux calculations derived from age models in Colman et al. (in press).

0.19%) in the core tops and decrease by less than 25% downcore. The TN values for these two cores indicate the possibility of a decreasing seaward trend in TN of surface sediments deposited in relatively shallow water (<10 m). Superimposed on the general downcore TN trends are several features of shorter duration. Cores RD98-P2, RR98-6, PX98-2, and PTMC-3 show stepwise reductions in TN downcore.

Like the TN results, ^{15}N shows consistent patterns when the cores are grouped by water depth. Measurements in cores RR98-6 and PX98-2 collected above the seasonal pycnocline decrease from about 8‰ at the tops of the cores to 5‰ at sediment depths of 50 cm. Average values remain around 5‰ to the bottoms of the cores. Values of ^{15}N from the tops of deep-water cores (RD98-P2, PRCK-3, PTMC-3) start near the shallow-water range (8‰ ±1.5) but decrease more gradually than in shallow-water cores (Appendix F). Rather than dropping sharply in the top 50 cm and then staying fairly constant like in the shallow-water cores, ^{15}N profiles from deep-water cores decrease over sediment depths of 150 to 300 cm and generally contain more variation than those from the shallow cores. Cores PTMC-3 and PRCK-3 are distinct in that, beginning at 175 cm, ^{15}N values increase downward for the rest of the core in the first case, and for the next 125 cm in the latter. The magnitude of the increase in PRCK-3 over this interval is greater than 2‰. There is no discernible seaward trend in ^{15}N data in either shallow-water or deep-water cores.

Carbon Isotopes, Total Organic Carbon, and C:N Ratio

Total organic carbon (TOC) in sediments and $^{13}C_{org}$ profiles for the five cores sampled are reported in Appendix F. Cores generally show a downward decrease in TOC in the top 1 to 3 m that stabilizes at about 0.75 to 1.2%. Because all of the OE facies and most of the RE facies consist of silty to sandy clays having relatively minor overall grain-size variation, grain size is not expected to be a major influence on TOC concentrations. TOC and TN are highly correlated with R^2 values ranging from 0.62 to 0.96 (excluding core RD98-P2) and an average C:N ratio of 8.8:1. The correlation is especially strong in cores PTMC-3, PRCK-3, and PX98-2 (Appendix F1-F3). Most measured C:N values that deviate by more than ±1.5 from the average ratio are the result of unusually high TOC values but TN values consistent with the rest of the data set. In particular, the RD98-P2 core has anomalously high TOC values between 75 and 175 cm that also result in unusually high C:N values (up to 14.7:1) over this interval (Appendix F6). On average, TOC decreases slightly from north to south and from deep to shallow water. Trends of C:N ratios increase slightly from north to south and from shallow to deep water, which is inconsistent with the expected decreasing contribution of terrestrial organic matter with increased distance from shore or downstream. The trends may result from different diagenetic processes in the water column and shallow sediment.

At both shallow and deepwater core sites, there is a seaward trend toward higher (less negative) $^{13}C_{org}$ values, indicating decreasing contribution of terrestrial organic matter, consistent with Hunt (1966). The average values for the northernmost cores (RD98-P2, -23.0‰; RR98-6,

-23.7‰) are 0.9-1.6‰ lower than for the southernmost core (PTMC-3, -22.1‰). There is also a shallow-water to deep-water gradient of increasing $^{13}C_{org}$ values. For example, the average $^{13}C_{org}$ of deep-water core RD98-P2 is 0.7‰ higher than that of the nearby shallow-water core RR98-6. The downcore variation from average $^{13}C_{org}$ values is about ±0.7‰ for deep-water cores and ±0.4‰ for shallow-water cores. The data suggest a slight downcore increase of <0.7‰ in $^{13}C_{org}$ at most sites.

Oxygen and Carbon Isotopes in Carbonate

Limited $^{13}C_{carb}$ and ^{18}O data were collected by analyzing foraminiferal calcite (*Elphidium sp.*) from two of the cores, PRCK-3 and PTMC-3 (Appendix F). The coarse resolution precludes detailed interpretation, but the overall trend in both cores is toward lower (more negative) $^{13}C_{carb}$ and ^{18}O values toward the core tops. The average $^{13}C_{carb}$ gradient is steeper in the PRCK-3 core (~0.50‰ m^{-1}) than in the PTMC-3 core (~0.13‰ m^{-1}). Lower ^{18}O values are consistent with greater input of fresh water and (or) reduced average salinity. The overall trends indicate general freshening of the bay that would be produced by increased runoff and/or gradual infilling of the basin. The difference between the two locations is greater than can be accounted for by differences in sedimentation rates and implies more rapid change overall at the northern core site (PRCK-3) closer to the mouth of the Susquehanna River. The slight trend toward higher $^{13}C_{org}$ in more recent sediments contrasts with the $^{13}C_{carb}$ and ^{18}O trends toward lower values.

DISCUSSION

We have applied a combination of the various geochemical proxies for past conditions in the Chesapeake Bay, an example of which is shown for the RD site south of Annapolis (Fig. 10). The upper panel shows a plot of biogenic silica flux, the middle panel shows data for nitrogen isotopes, and the lower panel presents authigenic rhenium flux for the site over the last 750 years (age scale from Colman *et al.*, in press). All three of these plots indicate that summer oxygen concentrations in Chesapeake Bay have fluctuated over time, including the pre-colonial period, but that anoxia began increasing steadily as early as 1775 A.D. and increased sharply around 1910. Diatom flux, and presumably overall productivity and nutrient loads, have increased by a factor of five over background levels. Nitrogen isotope values have increased by at least 3 ‰ indicating substantially more denitrification and anoxia in the bay. Rhenium fluxes have increased 4-fold with higher peaks. The beginning of these increases correlates with the advent of widespread agricultural development in the watershed and associated mobilization of nutrients with increased erosion. The increasing trends in anoxia indicators, however, do not yet appear to have stabilized or peaked, despite decreases in areas under cultivation, reduced nutrient loads, and trapping of sediments behind dams in the watershed.

CONCLUSIONS

The cores collected from Chesapeake Bay provide important information about how the bay evolved as an estuary and how it responds to sea-level change and Holocene climate fluctuations. They also provide information from which to evaluate the impact of humans on the watershed during the last few hundred years. In order to separate natural variability in the bay from human-induced changes, a variety of data sets are needed, including modern water quality, sediment lithologic variability, geochemical measurements, and micropaleontology. The data presented here focus on the sedimentological and geochemical measurements. Research in progress considers detailed interpretation of these data in terms of natural conditions, anthropogenic effects, and restoration efforts for Chesapeake Bay.

ACKNOWLEDGEMENTS

We thank R. Younger, captain of the R/V Kerhin, D. Nichols, and E. Mecray for assistance in collecting the cores discussed in this report. L. Ball, E. Grunwald, R. Murray, J. Yonehiro, and R. Ostermann helped with various aspects of the analytical work. Helpful reviews were provided by E. Mecray and L. Poppe.

REFERENCES

Böhlke, J.R., and Coplen, T.B., 1993, Interlaboratory comparison of reference materials for nitrogen-isotope-ratio measurements, *in* Reference and intercomparison materials for stable isotopes of light elements: International Atomic Energy Agency, IAEA-TECDOC-825, p. 51-66.

Brush, G.S., 1986, Geology and paleoecology of Chesapeake Bay: a long-term monitoring tool for management: Journal of the Washington Academy of Sciences, vol. 76, p. 146-160.

Carter, S.J., and Colman, S.M., 1994, Biogenic silica in Lake Baikal sediments: Results from 1990-1992 American cores: Journal of Great Lakes Research, vol. 20, p. 751-760.

Colman, S.M., and Mixon, R.B., 1988, The record of major sea-level fluctuations in a large Coastal Plain estuary, Chesapeake Bay, eastern United States: Palaeogeography, Palaeoclimatology, and Palaeoecology, vol. 68, p. 99-116.

Colman, S.M., Halka, J.P., Hobbs, C.H. III, Mixon R. B., Foster, D.S., 1990, Ancient channels of the Susquehanna River beneath Chesapeake Bay and the Delmarva Peninsula: Geological Society of America Bulletin, vol. 102, p. 1268-1279.

Colman, S.M., Bratton, J.F., and Baucom, P.C., 2000, Chapter 6. Radiocarbon dating of Marion-Dufresne cores MD99-2204, 2207, and 2209, Chesapeake Bay, *in* Cronin, T.M., Initial Report on IMAGES V Cruise of the Marion-Dufresne to the Chesapeake Bay June 20-22, 1999: U.S. Geological Survey Open-File Report 00-306, p. 72-77.

Colman, S.M., Baucom, P.C., Bratton, J., Cronin, T.M., McGeehin, J.P., Willard, D., Zimmerman, A., and Vogt, P., in press, Radiocarbon dating of Holocene sediments in Chesapeake Bay: Quaternary Research.

Cooper, S.R., 1995, Chesapeake Bay watershed historical land use: impact on water quality and diatom communities: Ecological Applications, vol. 5, p. 703-723.

Cooper, S.R., and Brush, G.S., 1991, Long-term history of Chesapeake Bay anoxia: Science, vol. 254, p. 992-996.

Cooper, S.R., and Brush, G.S., 1993, A 2,500-year history of anoxia and eutrophication in Chesapeake Bay: Estuaries, vol. 16, p. 617-626.

Cronin, T., Colman, S.M., Willard, D., Kerhin, R., Holmes, C., Karlsen, A., Ishman, S., and Bratton, J., 1999, Interdisciplinary environmental project probes Chesapeake Bay down to the core: EOS, Transactions of the American Geophysical Union, vol. 80, p. 237-241.

Cronin, T., Willard, D., Karlsen, A., Ishman, S., Verardo, S., McGeehin, J., Kerhin, R., Holmes, C., Colman, S.M., and Zimmerman, A., 2000, Climatic variability in the eastern United States over the past millenium from Chesapeake Bay sediments: Geology, vol. 28, p. 3-6.

Hicks, S.D., and Hickman, L.E., 1988, United States sea level variations through 1986: Shore and Beach, vol. 52, p. 3-7.

Hunt, J.M., 1966, The significance of carbon isotope variations in marine sediment: Advances in Organic Geochemistry, Second International Congress on Organic Geochemistry, p. 27-36.

Karlsen, A.W., Cronin, T.M., Ishman, S.E., Willard, D.A., Holmes, C.W., Marot, M., and Kerhin, R., 2001, Historical trends in Chesapeake Hay dissolved oxygen based on benthic foraminifera from sediment cores: Estuaries, 23, p. 488-508.

Kerhin, R.T., Williams, C., and Cronin, T.M., 1998, Lithologic descriptions of piston cores from Chesapeake Bay, Maryland: U.S. Geological Survey Open-File Report 98-787.

Mortlock, M.A., and Froelich, P.N., 1989, A simple method for rapid determination of biogenic opal in pelagic marine sediments: Deep-Sea Research, vol. 36, p. 1415-1426.

Murray, R.W. and Leinen, M., 1996, Scavenged excess Al and its relationship to bulk Ti in biogenic sediment from the central equatorial Pacific Ocean: Geochimica et Cosmochimica Acta, vol. 60, p. 3869-3878

Ostermann, D.R., and Curry, W.B., 2000, Calibration of stable isotopic data: An enriched ^{18}O standard used for source gas mixing detection and correction: Paleoceanography, vol. 15, p. 353–360.

Reynolds, R.L., and King, J.W., 1995, Magnetic records of climate change: Reviews of Geophysics, Supplement, vol. 78, p. 101-110.

Willard, D.A., and Korejwo, D., 2000, Chapter 7. Holocene palynology from *Marion-Dufresne* core MD99-2209 and 2207 from Chesapeake Bay: Impacts of climate and historic land-use change, *in* Cronin, T.M., ed., Initial Report on IMAGES V Cruise of the Marion-Dufresne to the Chesapeake Bay June 20-22, 1999: U.S. Geological Survey Open-File Report 00-306, p. 78-86.